Generation of a positively charged bubble and its possible mechanism of formation

M. Y. Han, M. K. Kim and M. S. Shin

ABSTRACT

The zeta potential of bubbles was measured in various solutions containing the metal ions Na^+, K^+, Ca^{2+}, Mg^{2+} and Al^{3+}. We discovered the main factors that can affect a bubble's zeta potential, resulting in a foundation for tailoring the zeta potential of bubbles during flotation processes. Bubbles were negatively charged in solutions of metal ions such as Na^+, K^+ and Ca^{2+} at every concentration and pH range studied. However, the magnitude of the zeta potential decreased with an increase in concentration and a decrease in pH value. Positively charged bubbles were observed in a solution of 0.01M $MgCl_2$ and an alkaline pH range, and below pH 8.2 with $AlCl_3$ in the concentration range of 10^{-5} to 10^{-2} M. Metal hydroxide precipitates affected the generation of positively charged bubbles, and minor hydroxylated species also contributed to increase the zeta potential of bubbles. Generation of positively charged bubbles could be the result of a combined mechanism, with both specific adsorption of hydroxylated species and precipitation of metal hydroxides on the bubble surface.

Key words | bubble charge, flotation, microbubbles, metal hydrolysis, metal precipitation, zeta potential

M. Y. Han (corresponding author)
M. K. Kim
The School of Civil, Urban & Geosystems
  Engineering,
Seoul National University,
Seoul 151-742,
Korea
E-mail: myhan@.snu.ac.kr;
  bmw337@snu.ac.kr

M. S. Shin
Eco-Frontier,
207-43, KAIST, Cheongryangri-dong,
Dongdaemoon-gu, Seoul 130-722,
Korea
E-mail: msshin@ecofrontier.co.kr

INTRODUCTION

Flotation is a separation process that uses small bubbles to remove low-density particles from water and wastewater treatment systems. The bubbles attach to fine particles in the water while rising to the surface. The characteristics of both the particle and the bubble (its size and surface charge) are important in determining the interactions between particles and bubbles.

A significant amount of work has been carried out to aid understanding of the characteristics of bubbles and the particle–bubble collision mechanism in the dissolved air flotation (DAF) process, and this work forms the basis of efficient design and operation of the DAF process (Edzwald *et al.* 1991; Edzwald 1995; Haarhoff & Edzwald 2004). However there is a need for additional research, especially on the subjects of bubble charge and how the bubble charge can be changed.

Han *et al.* (2001) has constructed a collision efficiency diagram, using trajectory analysis, that was used to calculate the collision efficiency for differential sedimentation (Han & Lawler 1991). The analysis considered the electrostatic interaction between particles and bubbles. It predicts high collision efficiency when the sizes of a particle and a bubble are similar and also when a particle and a bubble have opposite surface charge. Since the particle removal efficiency is affected by the collision efficiency between the particle and the bubble, Han *et al.* (2001) suggested that it might be possible to get higher efficiency by manipulating characteristics of both bubble and particle, instead of changing only the particle characteristics, which is generally accepted practice. In particular, use of a positively charged bubble may obviate the pretreatment of particles.

Although the zeta potential of particles in water is well documented, the zeta potential of bubbles has been measured only recently. Li & Somasundaran (1991 1992) measured the

zeta potential of nitrogen bubbles with sizes of 2–2.5 μm. However, in a typical electrophoresis method used to observe bubbles in a cell laid in a horizontal plane, only small bubbles can be measured because larger bubbles rise and disappear from focus. A major breakthrough has been made by rotating the cell and microscope through 90° and observing the cell and rising bubble in a vertical position. By doing this, the movement of large bubbles can be observed microscopically (Okada & Akagi 1987; Dockko *et al.* 1998; Kim *et al.* 2000; Han *et al.* 2004). The zeta potential of bubbles, like particles, is pH-dependent and negative at neutral pH (Okada & Akagi 1987; Dockko *et al.* 1998).
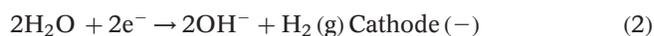
Production of a positively charged bubble has been reported in previous studies (Li & Somasundaran 1991; Malley 1995; Dockko *et al.* 1998; Kim *et al.* 2000; Han *et al.* 2004 2006). However, the discussions were incomplete and insufficient to establish how positive bubbles are generated by mono-, di- or trivalent metal ions and how positive bubbles attached to particles in the flotation process.

Therefore, the aims of this study are to examine conditions that generate positively charged bubbles in various metal solutions and to suggest a possible mechanism to explain the formation of positively charged bubbles.

METHODS AND MATERIALS

To measure the zeta potential of bubbles generated by electrolysis, we used an electrophoresis measurement (EPM) setup consisting of an electrophoresis cell, a microscope, a charge-coupled device (CCD) camera and a video image analyzer (Figure 1). The electrophoresis cell was made of two glass slides and its inner dimensions were 50 mm (length) × 40 mm (height) × 2 mm (width). The solution was added to or drawn from the opening top (2 mm (width) × 50 mm (length)). The platinum electrode (0.2 mm) was applied on the top and bottom of the cell. After inserting the target solution into the cell and then charging an instantaneous voltage on the top (+) and bottom (−), hydrogen and oxygen gas were generated by an electrochemical reaction. The gas bubbles were generated by the following redox reactions (Equations (1) and (2)) that occur at the platinum wires:

$$H_2O \rightarrow 2H^+ + \frac{1}{2} O_2\,(g) + 2e^-\,Anode\,(+) \qquad (1)$$

$$2H_2O + 2e^- \rightarrow 2OH^- + H_2\,(g)\,Cathode\,(-) \qquad (2)$$

Observation of bubble movement is easier for bubbles of smaller diameter because a large bubble has too high a velocity to measure. Therefore, in this study, we used hydrogen gas, which has a smaller bubble diameter (size range 15–65 μm, average size 22 μm) than oxygen (Han *et al.* 2002). The time taken by a hydrogen bubble to travel half the length of the cell after generation at the tip of the platinum wire is 5 s. All experiments were at the ambient temperature of 18–25 °C.
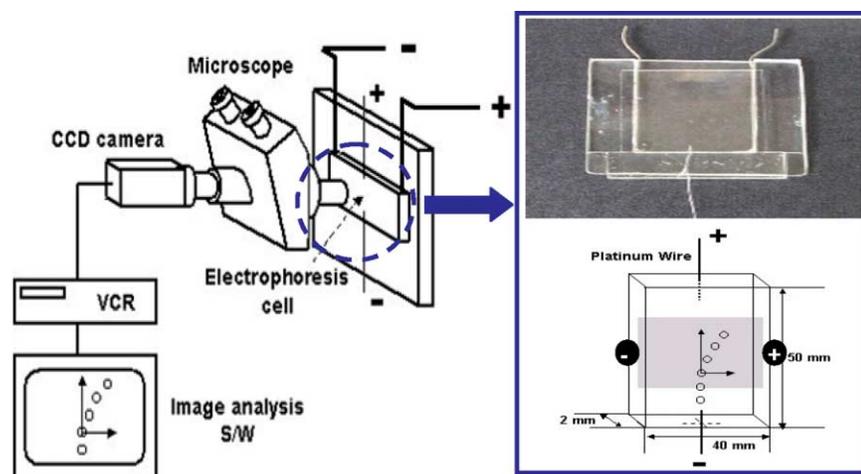

Figure 1 | Equipment for electrophoresis measurement.

Bubbles generated in the cell were photographed and recorded on a VCR attached to a CCD camera, as shown in Figure 1. When electric fields are applied to rising bubbles, they are deflected according to the sign of their charge. We derived the electrophoretic mobility from the velocity of the bubbles analyzed every 1/15 s and then calculated the zeta potential of bubbles with the Smoluchowski Equation (3):

$$\zeta = \frac{\eta V_e \lambda_o A}{\varepsilon_o \varepsilon_r i} \tag{3}$$

where

ζ = zeta potential (V);

η = viscosity (0.89×10^{-3} kg m^{-1} s^{-1}) at 25°C;

ε_o = the permittivity of a vacuum (8.854×10^{-12} kg^{-1} m^{-3} s^4 A^2);

ε_r = the relative permittivity (or dielectric constant = 78.5);

i = electric current (A);

λ_o = electrical conductivity of the solution (Ω^{-1} m^{-1});

A = cross-sectional area of the cell (m^2); and

V_e = velocity (m s^{-1}).

The electro-osmotic effect in a thin cell is a major practical problem in making electrophoresis measurements for zeta potential determinations. It is important to measure bubbles moving in the stationary layer. In order to avoid an electro-osmotic effect, the stationary level was derived from the equation below and we measured the velocities of the bubbles at this point (Collins *et al.* 1978). In this study, the microscope was focused on the stationary level in the cell and only bubbles showing a clear image on the videotape were measured:

$$y = \pm \frac{h}{\sqrt{3}} \tag{4}$$

where y is the position of the stationary layer from the midpoint of the cell (m); h is half the depth of the cell (m).

To create the desired solution conditions, five kinds of metal species (Na$^+$, K$^+$, Mg^{2+}, Ca^{2+}, Al^{3+}) were selected. To exclude the effect of the anion in the solutions of divalent and trivalent salts, the chloride salts were used throughout, dissolved in distilled water. Four different concentrations of metal ions were prepared, ranging from 10^{-5} M to 10^{-2} M in increments of one order. Solutions containing each metal ion, except potassium ions, were adjusted to the desired pH (from 3 to 12) by using hydrochloric acid and sodium hydroxide. In the case of the potassium ion, potassium hydroxide was used instead of sodium hydroxide. The experimental conditions are shown in Table 1.

To investigate the effect of hydrolytic substances of multivalent metals, magnesium and aluminum, on the zeta potential of bubbles, a 0.45 μm membrane filter (*Standard Methods* 1992; Tambo & Itoh 1977) was used to separate hydroxide precipitates of multivalent metals from each solution during the progress of experiments. A reasonable degree of removal of precipitate was confirmed by photos taken from the microscope before and after the membrane filtration.

RESULTS AND DISCUSSION

Zeta potential of bubbles in each solution

The zeta potential of bubbles in each solution (Table 1) is indicated in Figure 2. The zeta potential of bubbles in an NaCl solution was negative over the entire range of pH studied (Figure 2A). However, the magnitude of the zeta potential decreased with a decrease of pH. It has been reported that Na$^+$ and Cl$^-$ ions do not specifically adsorb at the gas–liquid interface (Li & Somasundaran 1991). It seems that Na$^+$ and Cl$^-$ ions are indifferent ions in this system. An indifferent ion can only extend the double layer of a colloid, consequently affecting the magnitude of zeta potential but not the sign (Hunter 1981).

Table 1 │ Experimental conditions for solutions

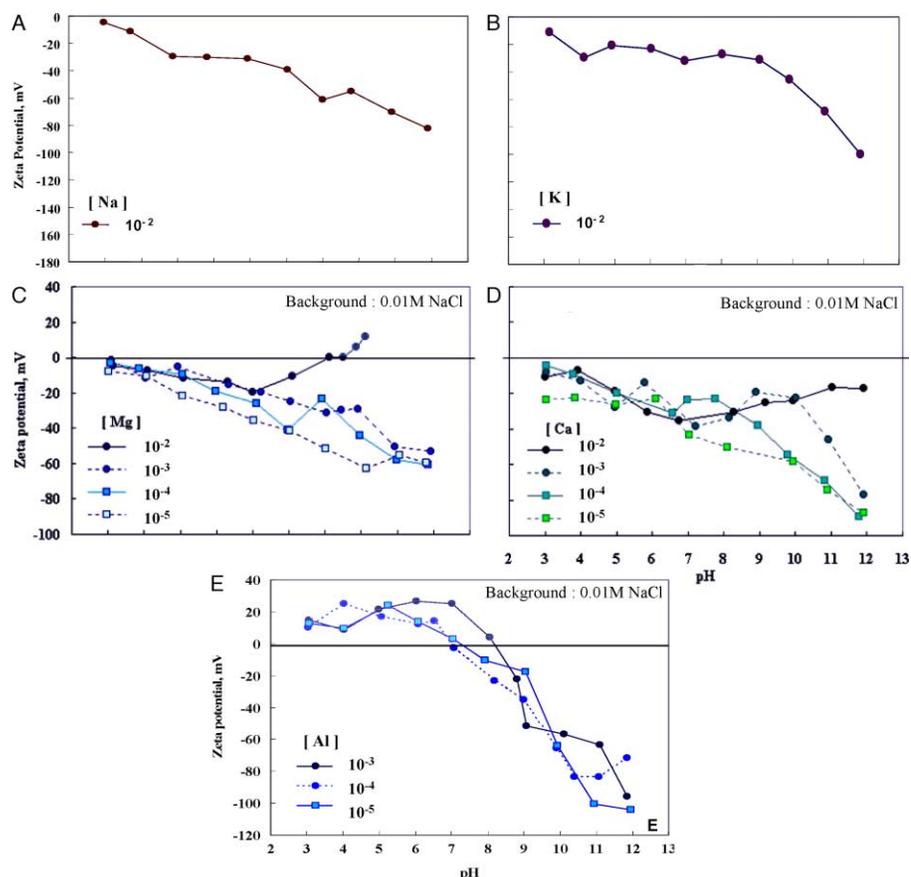| Valency of ion	Metal species	Concentration (M)
Monovalent	Na$^+$	10^{-2}
	K$^+$	10^{-2}
Divalent	Ca^{2+}	10^{-2}, 10^{-3}, 10^{-4}, 10^{-5}
	Mg^{2+}	10^{-2}, 10^{-3}, 10^{-4}, 10^{-5}
Trivalent	Al^{3+}	10^{-3}, 10^{-4}, 10^{-5}

Figure 2 | Zeta potential of bubbles in NaCl (A), KCl (B), MgCl$_2$ (C), CaCl$_2$ (D) and AlCl$_3$ (E) solutions (shaded areas indicate positive zeta potentials).

The zeta potential of bubbles in KCl varied with pH in almost the same way as sodium (Figure 2B). The bubble's zeta potential was negatively charged over the entire pH range, and the magnitude of the zeta potential decreased with a decrease of pH.

In the case of a MgCl$_2$ solution (Figure 2C), we observed positively charged bubbles above 0.01M MgCl$_2$ and in the alkaline pH region (marked as shaded in the graph). At acid pH, on the other hand, an increase of concentration caused a decrease in the magnitude of the bubble zeta potential.

The zeta potentials of bubbles in CaCl$_2$ solutions were negative throughout the entire experimental region (Figure 2D). However, the zeta potential of bubbles in 10^{-2} M CaCl$_2$ solution did not increase in negative value when the solution became alkaline (above pH = 7), but became less negative.

Positively charged bubbles were observed (Figure 2E) in AlCl$_3$ solutions of 10^{-5} M over a pH range of 3–7 (marked

as shaded on the graph). Increasing the AlCl$_3$ concentration to 10^{-3} M made the bubble more positively charged up to pH 8.2, with a maximum of about +30 mV. These results clearly show the powerful effect of aluminum ions on the electrokinetic behavior of the bubbles, relative to monovalent and divalent metal ions.

We could generate positively charged bubbles in the MgCl$_2$ solution of 10^{-2} M and in the AlCl$_3$ solutions of 10^{-3} M, 10^{-4} M, and 10^{-5} M. The critical aluminum concentration, 10^{-5} M, needed to reverse the zeta potential of bubbles was much lower than the corresponding magnesium concentration, 0.01M MgCl$_2$.

In order to identify the species involved in these effects of metal ions on the zeta potential of bubbles, we considered the magnesium, calcium and aluminum species distributions based on the thermodynamic equilibria of possible species (Table 2). For magnesium, Mg^{2+} and Mg(OH)$_{2(s)}$ are the predominant species in the lower and

Table 2 | Species distribution of magnesium, calcium, and aluminum according to pH at 25 °C

Item	pH	Major species	Minor species
$MgCl_2$	0–9	$MgCl_2 \rightarrow \mathbf{\underline{Mg^{2+}}} + 2Cl^- (pK^* = 11.41)$	$Mg(OH)^+$, $Mg(OH)_{2(s)}$
	9–14	$Mg^{2+} + 2OH^- \rightarrow \mathbf{\underline{Mg(OH)_{2(s)}}}(pK^* = 10.74)$	Mg^{2+}, $Mg(OH)^+$
$CaCl_2$	0–13	$CaCl_2 \rightarrow \mathbf{\underline{Ca^{2+}}} + 2Cl^- (pK^* = 12.67)$	$Ca(OH)^+$
	13–14	$Ca^{2+} + 2OH^- \rightarrow \mathbf{\underline{Ca(OH)_{2(s)}}}(pK^* = 5.26)$	$Ca(OH)^+$
$AlCl_3$	<5	$AlCl_3 \rightarrow \mathbf{\underline{Al^{3+}}} + 3Cl^- (pK^* = 4.98)$	$Al(OH)^{2+}$, $Al(OH)_2^+$, $Al(OH)_{(aq)}$, $Al(OH)_{3(s)}$, $Al(OH)_4^-$
	5–9	$Al^{3+} + 3OH^- \rightarrow \mathbf{\underline{Al(OH)_{3(s)}}}(pK^* = 32.9)$	Al^{3+}, $Al(OH)^{2+}$, $Al(OH)_2^+$, $Al(OH)_{(aq)}$, $Al(OH)_4^-$
	>9	$Al(OH)_{3(s)} + OH^- \rightarrow \mathbf{\underline{Al(OH)_4^-}}(pK^* = 12.35)$	Al^{3+}, $Al(OH)^{2+}$, $Al(OH)_2$, $Al(OH)_{(aq)}$, $Al(OH)_{3(s)}$

*Dean (1994).

higher pH regions, respectively. In the lower pH region in Figure 2C, the observed increase towards zero of the zeta potential is very likely due to the specific adsorption of Mg^{2+} ions at the gas–liquid interface.

With calcium, Ca^{2+} and $Ca(OH)_{2(s)}$ are the predominant species in the lower and higher pH regions, respectively (Table 2). $Ca(OH)_{2(s)}$ is a major species in the pH range 13–14, but can be disregarded because it is out of the pH region of interest. No positively charged bubbles were observed in the solution with calcium ions, so it is concluded that calcium ions can be expected to be inappropriate agents for altering the sign of the zeta potential below pH 12 (Figure 2D).

In the case of aluminum (Table 2), the solution pH has a significant effect on the species present, depending mainly on OH/Al ratio (Wang *et al.* 2004). In the acid pH region less than 5, there are three aluminum species to consider, namely Al^{3+}, $Al(OH)_{3(s)}$, and $Al(OH)_4^-$, but Al^{3+} is the predominant species. The bubbles are positively charged in the presence of $AlCl_3$ in this region, as illustrated in Figure 2E.

In the pH region of 5–9, where $Al(OH)_{3(s)}$ is the predominant species, the bubbles had a positive zeta potential or were near zero. As the $AlCl_3$ concentration increased up to 0.001M $AlCl_3$, the magnitude of the zeta potential increased as shown in Figure 2E. Accordingly, it could be stated that aluminum hydroxide precipitates maintain the bubble's positive zeta potential.

In the alkaline pH region >9, $Al(OH)_4^-$ is the primary species, which causes the zeta potential of the bubble to be more negative than in their absence. It seems that OH^- may be the main determinant of negative bubble charge.

As the $AlCl_3$ concentration was increased, the zeta potential of the bubble eventually turned positive above a certain concentration. The charge reversal in this zone seems to be attributable to the adsorption of Al^{3+} ions at the gas–liquid interface. Compared with the adsorbing capacity of other ionic species, the aluminum ion can be said to adsorb specifically onto the bubble interface more successfully because of its high valency.

The effect of metal hydroxide precipitates

To investigate the effect of metal hydroxide precipitates on the zeta potential of bubbles, the zeta potential of $Mg(OH)_{2(s)}$ and $Al(OH)_{3(s)}$ were measured. In the case of $CaCl_2$, $Ca(OH)_{2(s)}$ was not detected in the pH range of this study.

To comprehend the mechanism of charge reversal by hydroxide precipitates, we compared two conditions, one with and one without a precipitate. The zeta potential with and without $Mg(OH)_{2(s)}$ is shown in Figure 3A. The zeta potential of the bubble was negative and increased in value as pH increased when $Mg(OH)_{2(s)}$ was absent at 10^{-2} M $MgCl_2$. Therefore, $Mg(OH)_{2(s)}$ seems to be a critical factor controlling the sign of the zeta potential. Moreover, the zeta potential of $Mg(OH)_{2(s)}$ was measured as shown in
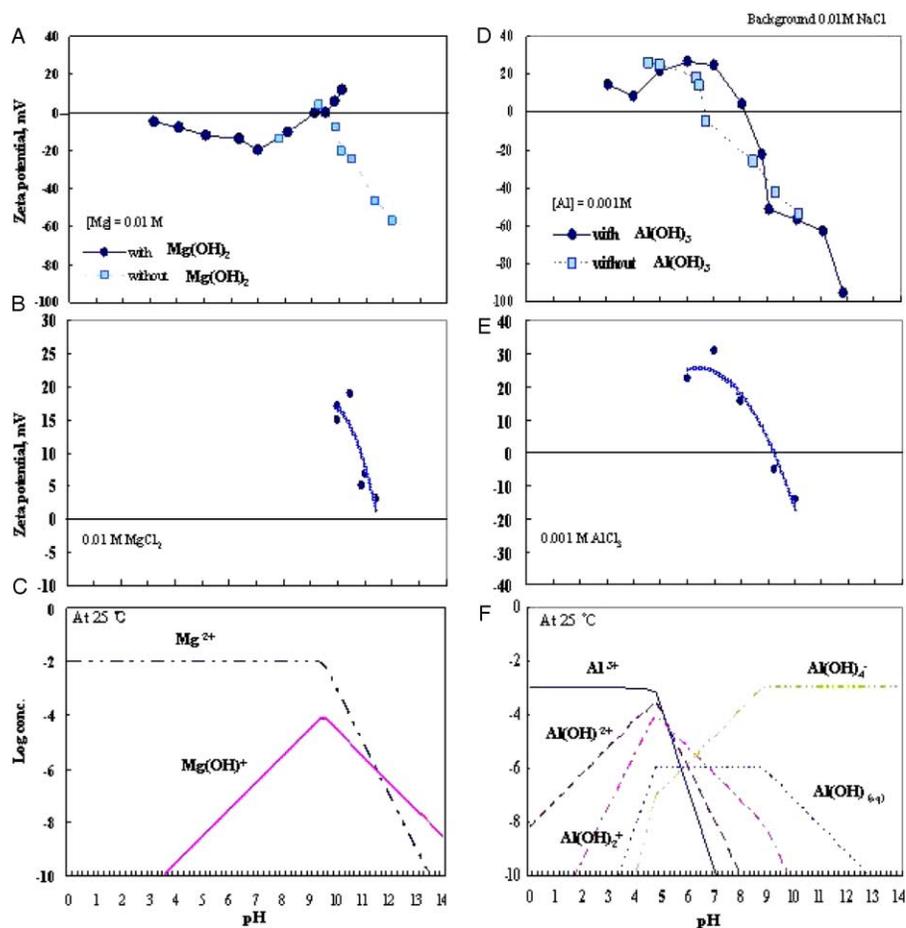
Figure 3 │ Effect of hydroxide precipitates, Mg(OH)$_{2(s)}$ and Al(OH)$_{3(s)}$ on zeta potential of bubbles as a function of pH (A and D – zeta potential of bubbles with and without Mg(OH)$_{2(s)}$ and Al(OH)$_{3(s)}$, B and E – zeta potential of Mg(OH)$_{2(s)}$ and Al(OH)$_{3(s)}$, C and F – log concentration of Mg and Al species as a function of pH except Mg(OH)$_{2(s)}$ and Al(OH)$_{3(s)}$).

Figure 3B. Mg(OH)$_{2(s)}$ was positively charged in the alkaline pH region at a concentration of 0.01M MgCl$_2$, and the magnitude of the zeta potential decreased with an increase of pH. Therefore, the positively charged bubble in 0.01 M MgCl$_2$ solution can be attributed to the presence of positively charged Mg(OH)$_{2(s)}$.

In addition, we observed that the zeta potential of a bubble approached the zero zeta potential line without Mg(OH)$_{2(s)}$. When a pH was reached at which some of the lower-charged hydroxylated species (i.e. Mg(OH)$^+$) began to appear, the zeta potential of the bubble increased in positive value, as shown in Figure 3C. When the concentration of the Mg(OH)$^+$ species decreased, the bubble's zeta potential showed definite negative charge.

In AlCl$_3$ solution, the zeta potential of bubbles was positive in the neutral pH region (Figure 3E), where

Al(OH)$_{3(s)}$ was the predominant species. Since Al(OH)$_{3(s)}$ has a positive charge below around pH 9, charge reversal of a bubble in the neutral pH region seems to result from the presence of positively charged aluminum hydroxide precipitates.

The effect of aluminum hydroxide precipitate is shown in Figure 3D. When aluminum hydroxide precipitates were removed, the isoelectric point of the bubble was shifted into the acid pH region. In other words, the region for positively charged bubbles was narrow compared with the situation with Al(OH)$_{3(s)}$. In the acid pH region, the magnitude of positively charged bubbles was hardly affected by the presence of Al(OH)$_{3(s)}$ because the main species in this region is the free aluminum ion. However, the zeta potential of the bubbles began to decrease toward negative values in the neutral pH region without hydroxide precipitates.
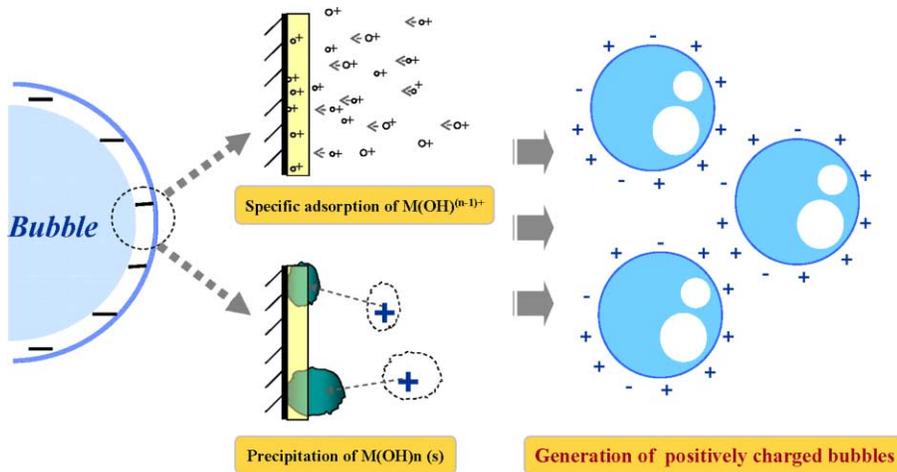
Figure 4 │ Probable principle explaining the procedure of charge reversal.

Considering that $Al(OH)_{3(s)}$ is a major species at neutral pH, these amorphous solids could be considered important species for maintaining the bubble at a positive zeta potential.

At the same time, there are several minor species, including $Al(OH)_2^+$, $Al(OH)_{3(aq)}$ and $Al(OH)^{2+}$, that were present, as shown in Figure 3F. Considering that the zeta potential of a bubble was still positive without $Al(OH)_{3(s)}$, these soluble hydroxylated species also seemed to play a role in the production of positively charged bubbles.

Proposed model for positively charged bubbles

Previous investigators (Brandon *et al.* 1985; Okada & Akagi 1987; Li & Somasundaran 1991; Dockko *et al.* 1998) showed that the bubble has a negative charge at neutral pH. Some found that the charge can be changed to be positive by chemical addition or pH adjustment (Li & Somasundaran 1991; Dockko *et al.* 1998).

From the above results, we suggest a probable principle of how positively charged bubbles are generated. We suggest a combined mechanism, with both specific adsorption of hydroxylated species and formation of hydroxide precipitates (Figure 4). Consequently, a prior knowledge of metal species distribution and solution conditions could lead to a tailoring of the zeta potential of bubbles in a flotation process.

Trivalent ions seem to be more useful than divalent ones if positively charged bubbles need to be generated in flotation. Moreover, addition of aluminum ions seems to be a reasonable way to make positively charged bubbles because a strongly alkaline solution is necessary to generate a positive zeta potential utilizing magnesium ions.

Han *et al.* (2006) has verified modeling by experiments that demonstrate that the removal efficiency between bubble and particle is greater when the zeta potential of one is negative and that of the other is positive. Therefore, effective and selective removal of suspended particles could be made practicable by generating bubbles with the desired charge, making allowances for the sign and magnitude of the zeta potential of the particle as well.

CONCLUSIONS

This study was performed to measure the zeta potential of bubbles in various solutions containing metal ions and to discover the main factors that can affect the zeta potential. The zeta potential of bubbles in NaCl, KCl, and $CaCl_2$ solutions was negative over the entire range of concentrations and pH. However, the magnitude of the zeta potential decreased with an increase in concentration and a decrease in pH value. Positively charged bubbles were observed in the solution of 0.01M $MgCl_2$ in the alkaline pH range, and over the range pH 3–8.2 and 10^{-5} to 10^{-2} M $AlCl_3$. In the cases of magnesium and aluminum solutions, metal hydroxide precipitates affected positive bubble generation and minor hydroxylated species also contributed

to increasing the zeta potential of the bubble. Therefore, the generation of positive bubbles could be explained by a combined mechanism, with both specific adsorption of hydroxylated species and precipitation of hydroxides. It also depended on the metal ion concentration in the solution. Consequently, a prior knowledge of metal species distribution and solution conditions could lead to a tailoring of the zeta potential of bubbles in the flotation process. Through this procedure, effective and selective removal of suspended particles could be made practicable by generating bubbles with the desired charge, making allowances for the sign and magnitude of the particle zeta potential as well.

ACKNOWLEDGEMENTS

REFERENCES

Brandon, N. P., Kelsall, G. H., Levine, S. & Smith, A. L. 1985 Interfacial electrical properties of electrogenerated bubbles. *J. Appl. Electrochem.* **15**, 485–493.

Collins, G. L., Motarjemi, M. & Jameson, G. J. 1978 A method for measuring the charge on small gas bubbles. *J. Colloid Interface Sci.* **63**(1), 69–75.

Dean, J. A. 1994 *Lange's Handbook of Chemistry*, 14th edn. McGraw-Hill, New York, pp. 8.6–8.18.

Dockko, S., Han, M. Y. & Park, C. H. 1998 Measuring zeta potential of microbubbles in DAF. *J. Korean Soc. Wat. Wastewat* **12**(4), 53–58.

Edzwald, J. K. 1995 Principles and applications of dissolved air flotation. *Wat. Sci. Technol.* **31**(3–4), 1–23.

Edzwald, J. K., Malley, J. P., Jr & Yu, C. 1991 A conceptual model for dissolved air flotation in water treatment. *Wat. Supply* **9**(1), 141–150.

Haarhoff, J. & Edzwald, J. K. 2004 Dissolved air flotation modelling: insights and shortcomings. *J. Wat. Supply Res. Technol. – Aqua* **53**(3), 127–150.

Han, M. Y., Ahn, H. J., Shin, M. S. & Kim, S. R. 2004 The effect of divalent metal ion on the zeta potential of bubbles. *Wat. Sci. Technol.* **50**(8), 49–56.

Han, M. Y., Kim, M. K. & Ahn, H. J. 2006 Effects of surface charge, microbubble size and particle size on removal efficiency of electro-flotation. *Wat. Sci. Technol.* **53**(7), 127–132.

Han, M. Y., Kim, W. T. & Dockko, S. 2001 Collision efficiency factor of bubble and particle (αbp) in DAF: theory and experimental verification. *Wat. Sci. Technol.* **43**(8), 139–144.

Han, M. Y. & Lawler, D. F. 1991 Interaction of two settling spheres: settling rates and collision efficiencies. *J. Hydraul. Engng. ASCE* **117**(10), 1269–1289.

Han, M. Y., Park, Y. H. & Yu, T. J. 2002 Development of a new method of measuring bubble size. *Wat. Sci. Technol. Wat. Supply* **2**(2), 77–83.

Hunter, R. J. 1981 *Zeta Potential in Colloid Science*. Academic Press, New York.

Kim, W. T., Han, M. Y., Lee, S. W. & Han, Y. S. 2000 Zeta potential measurement of micro bubble generated by electroflotation (in Korean). *J. Korean Soc. Wat. Wastewat.* **14**(4), 343–349.

Li, C. & Somasundaran, P. 1991 Reversal of bubble charge in multivalent inorganic salt solution: effect of magnesium. *J. Colloid Interface Sci.* **146**(1), 215–218.

Li, C. & Somasundaran, P. 1992 Reversal of bubble charge in multivalent inorganic salt solution: effect of aluminum. *J. Colloid Interface Sci.* **148**(2), 587–591.

Malley, J. P., Jr 1995 The use of selective and direct DAF for removal of particulate contaminants in drinking water and treatment. *Wat. Sci. Technol.* **31**(3–4), 49–57.

Okada, K. & Akagi, Y. 1987 Method and apparatus to measure the zeta potential of bubbles. *J. Chem. Engng. Japan* **20**(1), 11–15.

Standard Methods for the Examination of Water and Wastewater 1992 18th edn. APHA/AWWA/WEF, Washington, DC.

Tambo, N. & Itoh, H. 1977 Electrophoretic studies on natural color colloid coagulation by aluminum. *J. Japan Wat. Works Assoc.* **508**, 38.

Wang Donsheng,, Sun, W., Xu, Y., Tang, H. & Gregory, J. 2004 Speciation stability of inorganic polymer flocculant-PACl. *Coll. Surfaces A: Physicochem. Engng. Aspects* **246**, 1–10.